SUPPORTING MATERIAL

Lipopolysaccharide-induced dynamic lipid membrane reorganization: tubules, perforations and stacks

Peter G. Adams[†], Loreen Lamoureux[‡], Kirstie L. Swingle[†§], Harshini Mukundan[¶‖], Gabriel A. Montaño[†*]

[†] Center for Integrated Nanotechnologies, Los Alamos National Laboratory, Los Alamos, NM, 87545. [‡] Center for Biomedical Engineering, University of New Mexico, Albuquerque, NM, 87131. [§] Department of Biology, University of New Mexico, Albuquerque, NM 87131. [¶] New Mexico Consortium, Los Alamos, NM, 87545. [‖] Physical Chemistry and Applied Spectroscopy, Los Alamos National Laboratory, Los Alamos, NM, 87545.

Eight figures S1 – S8 and legends

Legends for four movies S1 – S4.

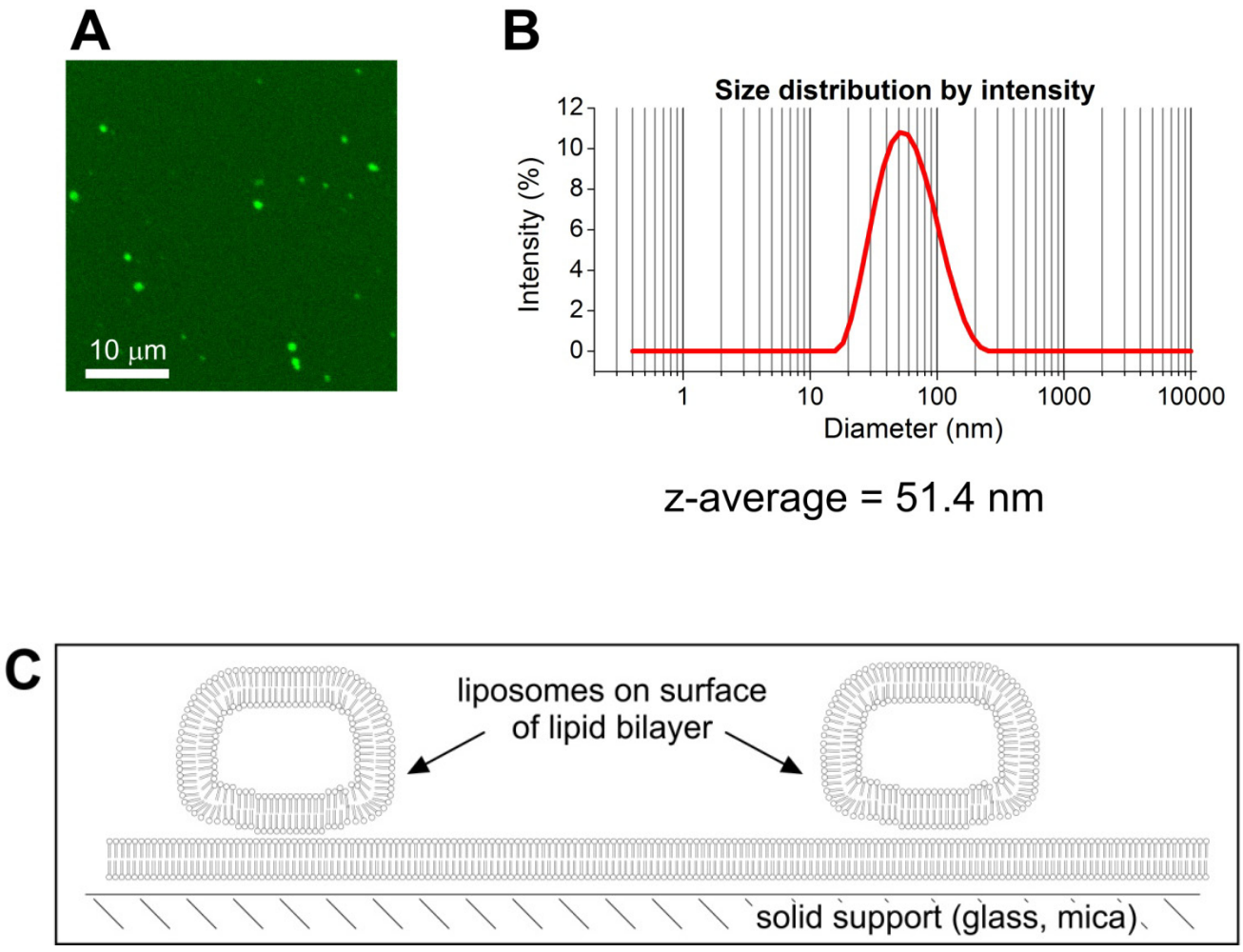

FIGURE S1 Size of surface-associated lipid vesicles. (A) Representative LSCM image of surface associated vesicles. See Movie S1 for mobility data. (B) Representative dynamic light scattering size distribution (by intensity). (C) Schematic showing proposed surface associated vesicles.

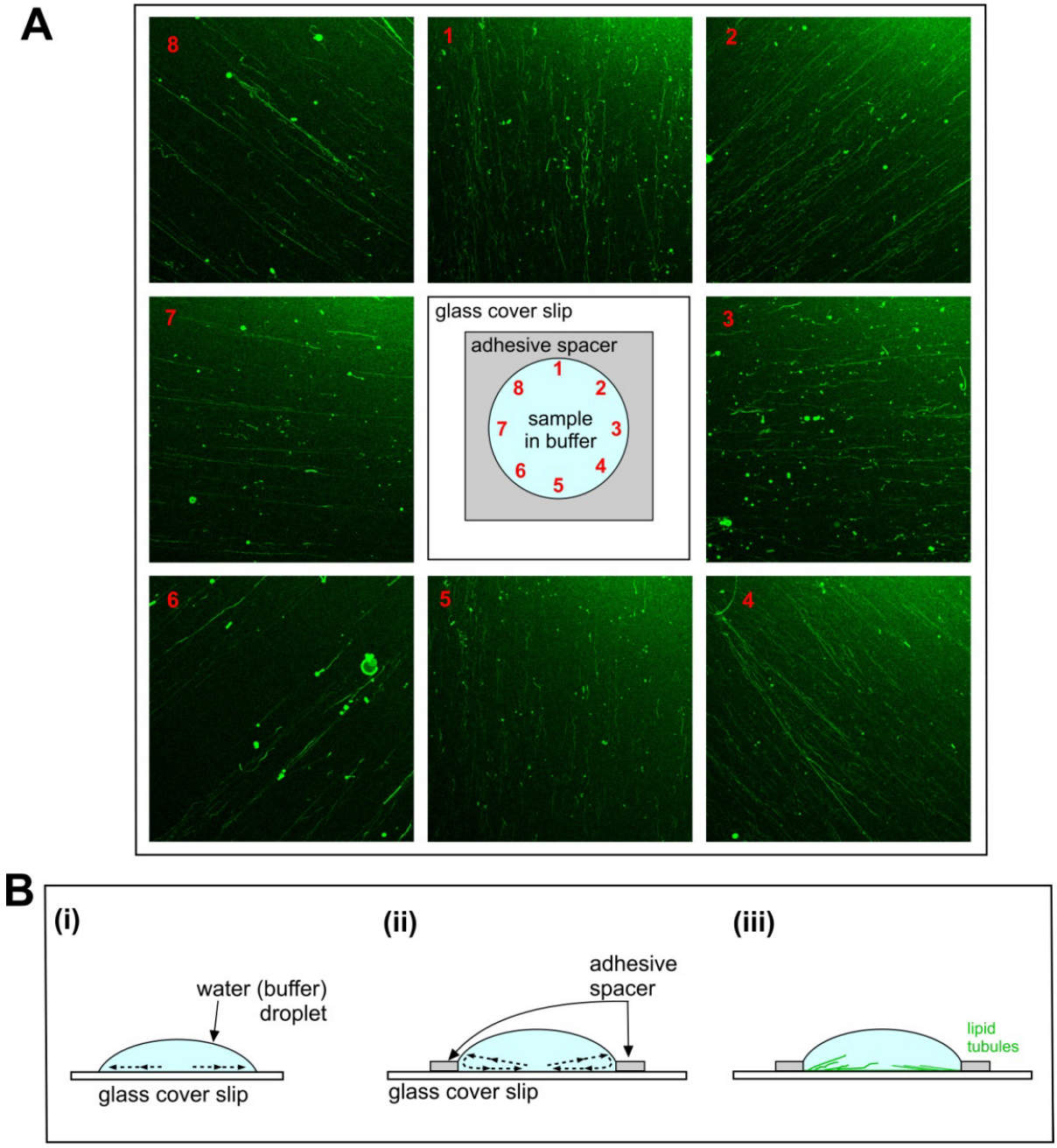

FIGURE S2 Elongation of lipid tubules. (A) LSCM fluorescence images acquired of the radial pattern formed by lipid tubules at the edges of the buffer droplet (images 1-8, position labeled on the schematic sample set-up and on the images). A DOPC sLBA (0.5% BODIPY lipids) in PBS was treated with 100 μg/mL LPS and then images of tubules extending above the sLBA were acquired after approximately 30 min. The tubules were most evident by focusing approximately 2 μm above the surface. (B) Cartoon of possible convection currents causing flow within the buffer droplets. (i) A droplet of water is expected to cause flow in the direction toward the edges of the droplet, driven by evaporation, similar to the "coffee-ring effect". (ii) Our open droplet set-up, with an imaging spacer which creates boundary walls to the droplet. Complex buffer flows and counter-flows may exist. (iii) These currents serve to stretch out the lipid tubules formed by LPS.

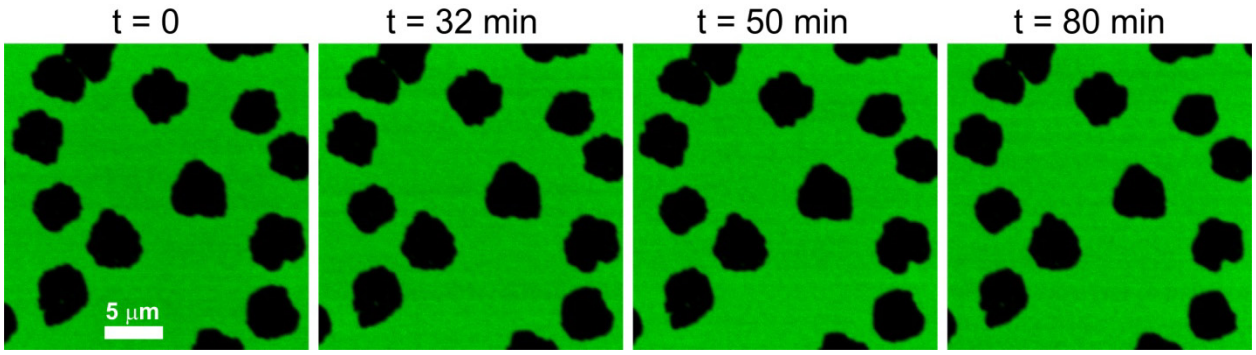

FIGURE S3 Fluorescence time-course showing that holes are stable. Time lapse LSCM fluorescence images over the course of 80 min showing the size and shape of holes within the lipid bilayer after LPS treatment. There are no significant changes in the holes.

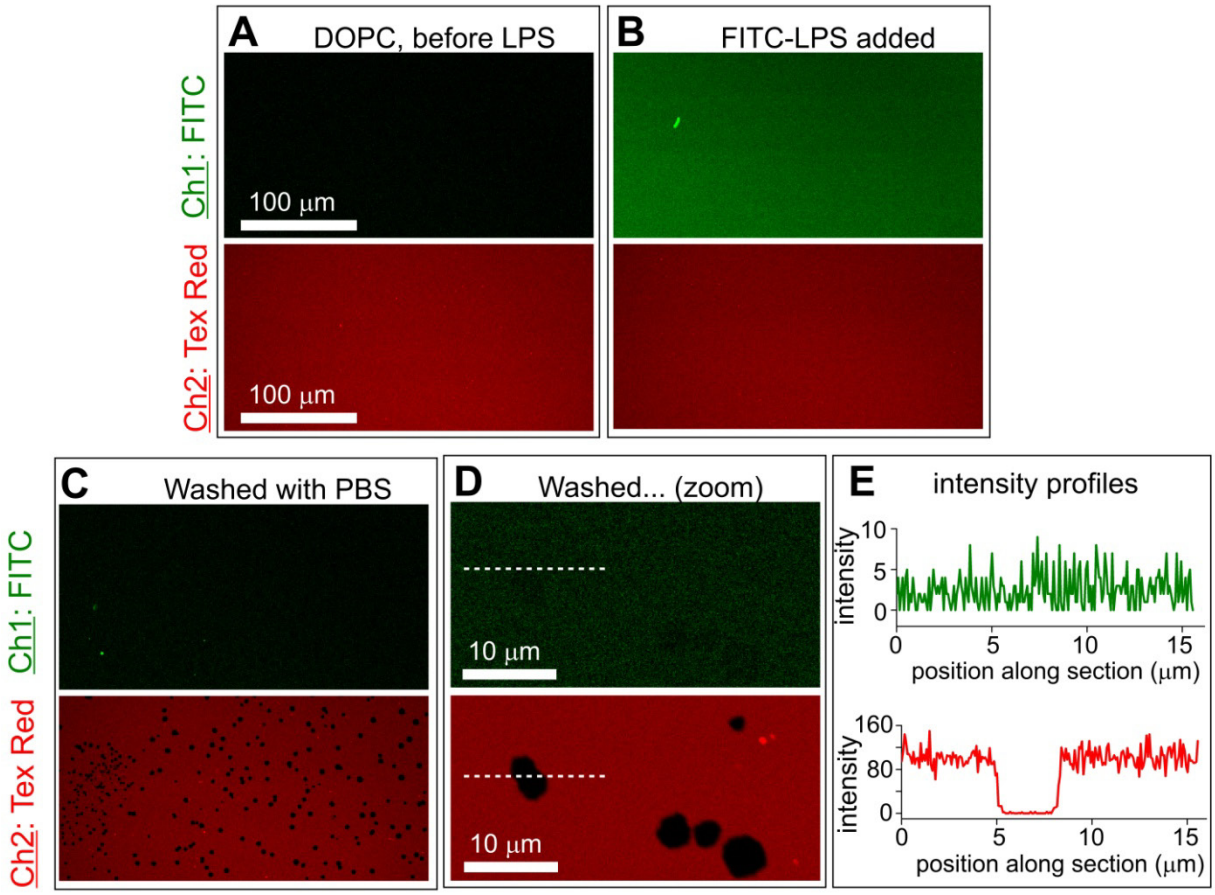

FIGURE S4 Dual channel LSCM fluorescence images tracking FITC-LPS its hole formation. *Upper panels*: signal from the FITC-LPS (505-525 nm range); *lower panels*: signal from the DOPC bilayer doped with 0.5% Texas Red fluorescent lipids (655-755 nm range). Images are shown, (A) before LPS addition, (B) after addition of 100 μg/ mL FITC-LPS in PBS, (C) after 500 μg/ mL FITC-LPS treatment and washing the surface with ten changes of PBS. (D) A higher magnification image from (C), and (E) intensity profiles revealed voids in the Texas Red lipid fluorescence but very low FITC signal with no observable signal difference on or off the holes observed in the matched Texas Red channel.

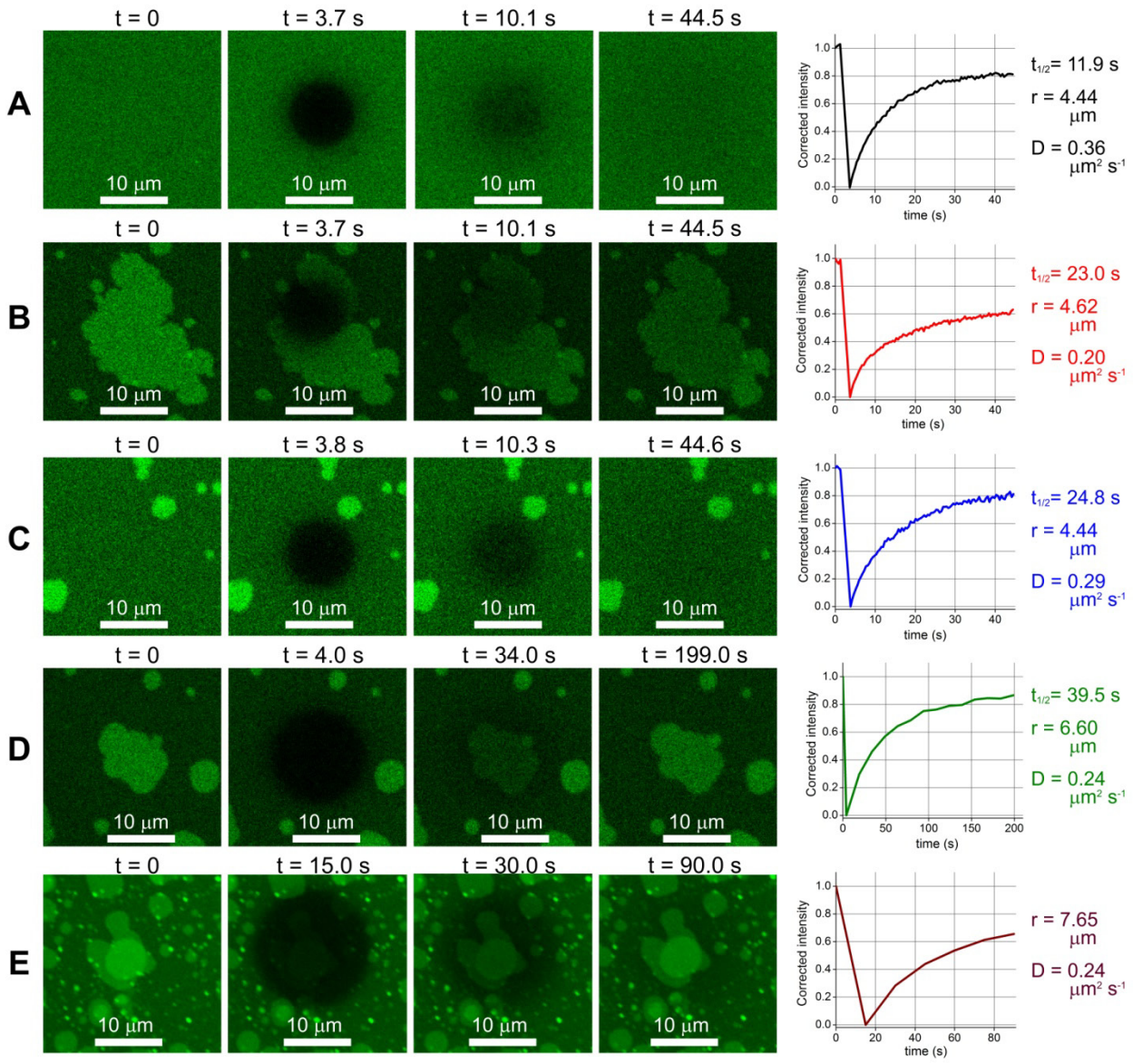

FIGURE S5 FRAP studies on LPS (Ca^{2+}) planar lamellar sheets. (A) FRAP of a normal DOPC sLBA in Ca^{2+} buffer. (B) FRAP of a planar lamellar sheet after LPS (Ca^{2+}) treatment. (C) FRAP of the sLBA (nearby planar sheets visible) after LPS (Ca^{2+}) treatment. (D) FRAP after bleaching an entire single-layer lamellar sheet. (E) FRAP after bleaching an entire multi-layer lamellar sheet. The corrected intensity vs. time plots show the fluorescence recovery over time in the bleached region. The first measurement post-bleach intensity in the ROI was normalized to zero, correction for any unintended photobleaching over the image series was made* and the data set was normalized to the pre-bleach intensity (intensity = 1 at t= 0). *by multiplication of each intensity measurement in the bleach ROI by F_{pre}/F_{post} in a region of the image that was *not* bleached, where F_{pre}= prebleach intensity (t= 0) and = F_{post} postbleach intensity at each time point. The recovery half-time ($t_{(1/2)}$) was measured from the plots. Diffusions coefficients were then calculated using the formula "$D = 0.22.r^2 / t_{(1/2)}$" (r = radius of bleached area).

The diffusion coefficients for the sLBA are similar with a possible slight reduction after LPS(Ca^{2+}) treatment. The diffusion coefficient for the planar sheet is significantly lower than that for the sLBA. The diffusion coefficients for bleaching an entire single or multi-lamellar planar sheet are intermediate values.

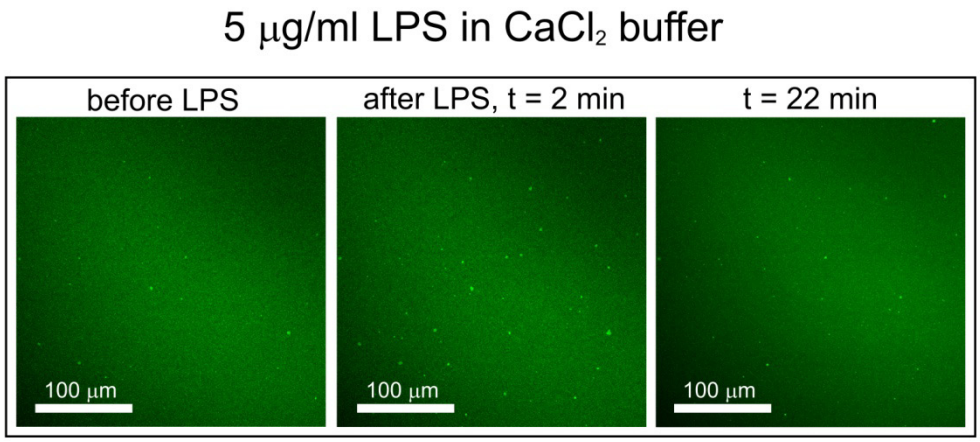

FIGURE S6 LPS concentration dependence of planar sheet formation. LSCM fluorescence images of an sLBA before and after addition of 5 μg/ mL LPS in Ca^{2+} buffer. Sequential images are shown after 2 min and 22 min after addition of the LPS.

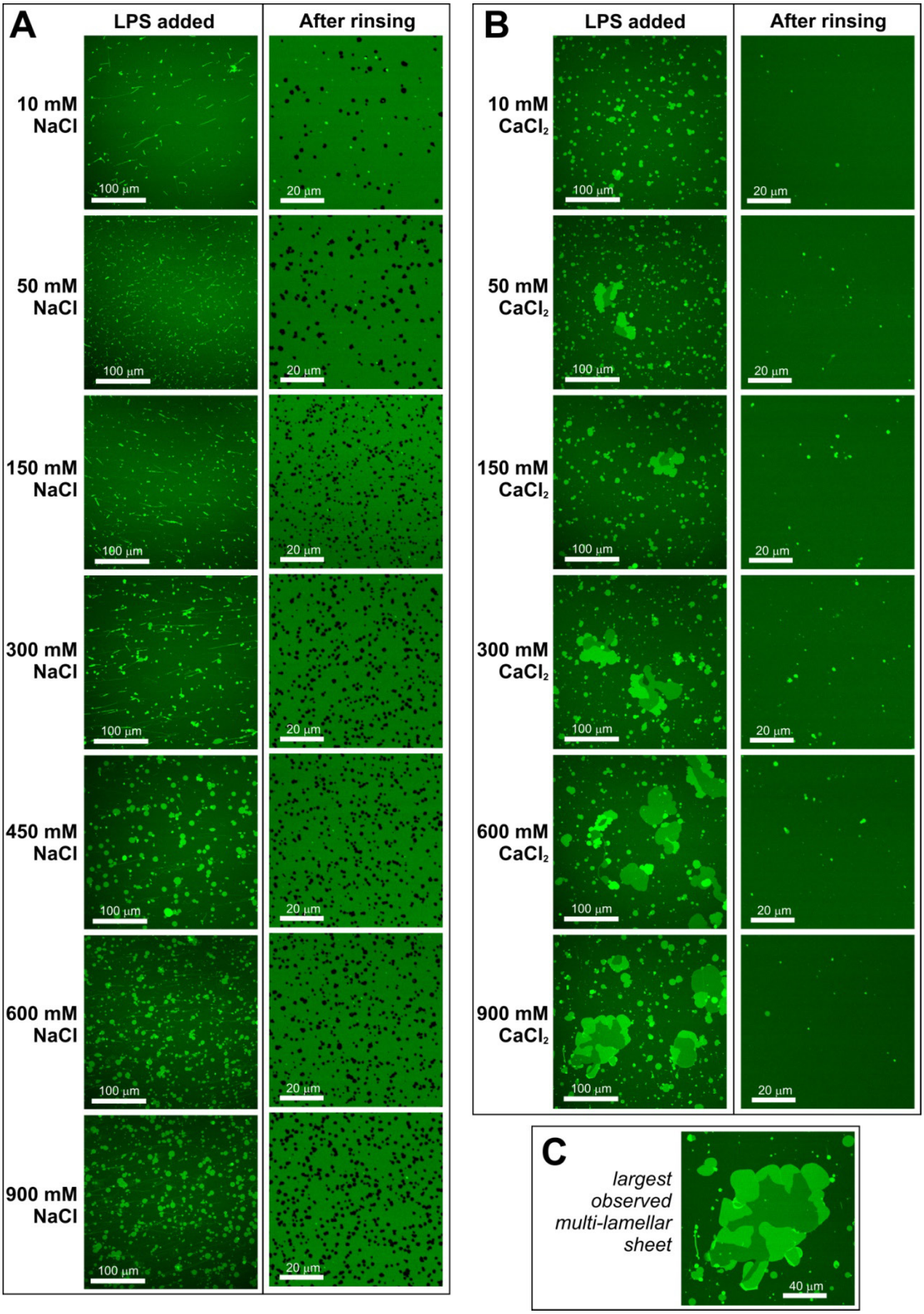

FIGURE S7 Cation concentration effects on LPS membrane disruption. (A) Representative LSCM images from showing the effects of LPS in a series of buffers with increasing NaCl concentration. All buffers contained 20 mM TRIS (pH 7.5). sLBAs were treated with 100 µg/ mL LPS and imaged after approximately 15 min after LPS addition (column 1) and after rinsing the surface with fresh buffer (column 2). (B) As in (A), except using a buffer series with $CaCl_2$ instead of NaCl. (C) The largest multilamellar lipid patch observed.

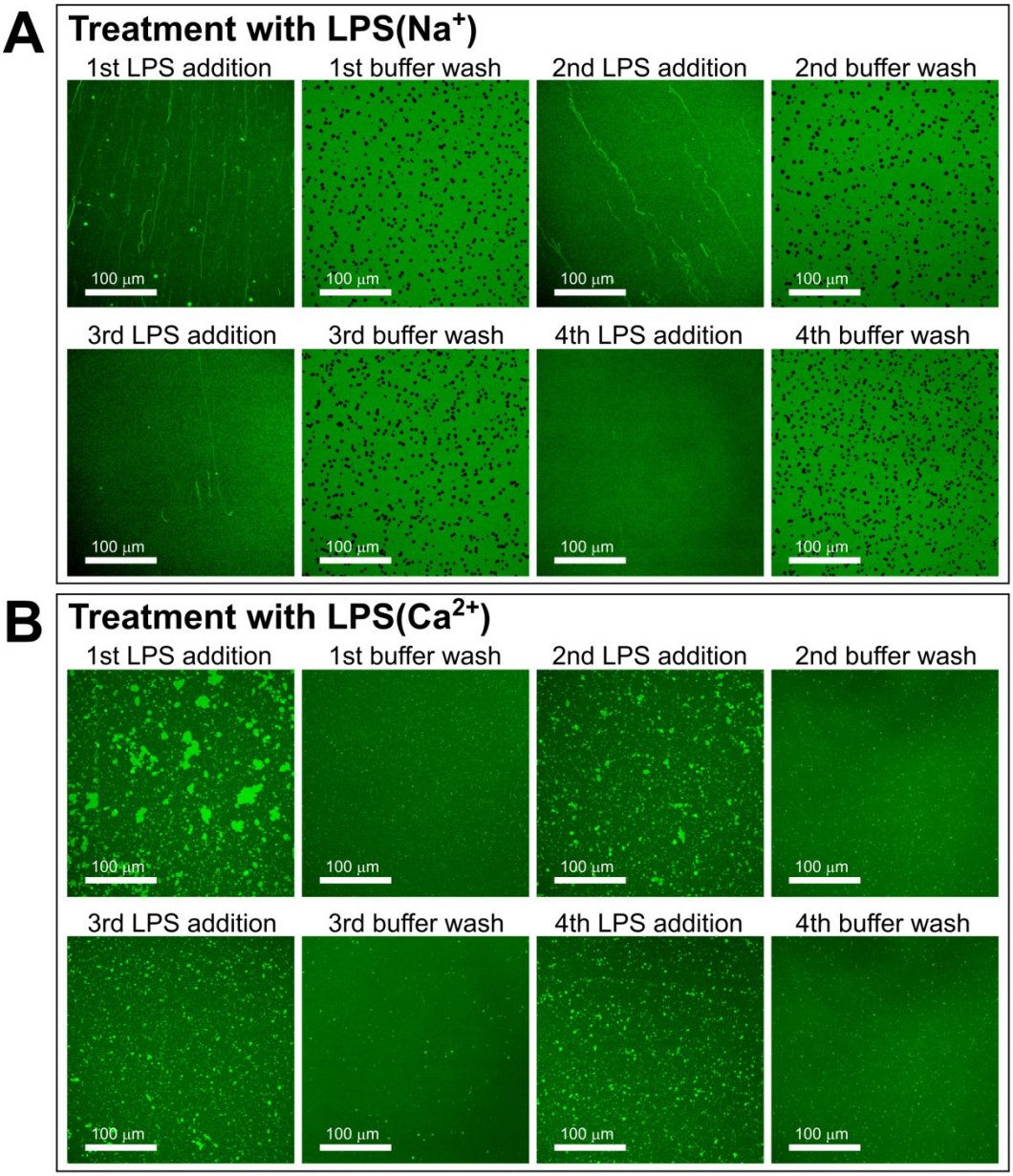

FIGURE S8 (A) Reduction in lipid tubules and similar hole formation by multiple cycles of LPS treatment. DOPC sLBAs were incubated with 100 µg/ mL LPS in PBS for 20 min, LSCM images acquired of lipid tubules and then washed with PBS and imaged again. This was repeated until 4 cycles of LPS treatment had been performed. After each LPS treatment lipid tubules were formed and then removed during the buffer wash. Fewer tubules were observed with each LPS treatment, due to the expected depletion of surface-associated vesicles. Note that holes were formed after the first buffer wash and then 'filled-in' by the 2nd LPS treatment, probably due to packing of LPS into the holes, joining up with the lipid bilayer, allowing lateral lipid diffusion and 'healing' of the holes. However, following the each buffer wash, holes of a similar size and distribution were formed once again, suggesting that hole formation does not depend on surface-associated vesicles, but on the solid-supported lipid bilayer and interaction with LPS.
(B) Reduction in planar sheet formation by multiple cycles of LPS treatment. DOPC sLBAs were incubated with 100 µg/ mL LPS in Ca^{2+} buffer for 20 min, LSCM images acquired of planar sheets and then washed with Ca^{2+} buffer and imaged again. This was repeated until 4 cycles of LPS treatment had been performed. Not all sheets are removed by each buffer wash, but there is a trend to form smaller and fewer planar lamellar sheets with each subsequent LPS treatment.

MOVIE S1 Mobility of surface-associated lipid vesicles. Time-lapse LSCM series of images showing the motion of surface-associated vesicles on a DOPC sLBA. Total image represents 39.4 x 39.4 μm, interval between images is 1.0 s

MOVIE S2 Lipid tubule formation. Time-lapse LSCM series of images showing treatment of a DOPC sLBA with 100 μg/ mL LPS in PBS. Total image represents 105.3 x 105.3 μm. Series 1 was acquired with continuous image acquisition (1.1 s/ image, no interval) and the droplet of LPS is added to the sample at ~10 s (Series 1). Series 2 was then acquired on the same field, with an interval of 15 s, to allow slower processes to be observed. Elapsed time for each series is shown as "T #seconds # milliseconds". Each image series was contrast-adjusted independently for clarity. Disordered lipid tubules are formed immediately after LPS addition and they extended and stretch out over the course of Series 1 and 2. Note, the overall fluorescence signal is reduced between images "9 s 981 ms" and "12 s 199 ms" (Series 1) because of slight defocusing of the sample due to the physical effect of adding the droplet of LPS at ~10 s. Refocusing on the sLBA after imaging reveals a similar sLBA fluorescence before and after LPS addition.

MOVIE S3 Lipid tubule mobility. Epifluorescence 'movie' imaging of a DOPC sLBA after ~20 min treatment with 100 μg/ mL LPS in PBS. Total image represents 132 x 132 μm. High lateral mobility of lipid tubules is apparent.

MOVIE S4 Lipid sheet formation and growth. Time-lapse LSCM series of images showing treatment of a DOPC sLBA with 100 μg/ mL LPS in Ca^{2+} buffer. Total image width represents 317.3 x 317.3 μm. Series 1 was acquired with continuous image acquisition (3.3 s/ image, no interval) and the droplet of LPS is added to the sample at ~9 s (Series 1). Series 2 was then acquired on the same field, after refocusing (3.3 s/ image, no interval). Series 3 was then acquired with an interval of 30 s, to allow slower processes to be observed. Elapsed time for each series is shown as "T #seconds # milliseconds". Each image series was contrast-adjusted independently for clarity. Patches of fluorescence, expected to represent planar lipid/LPS lamellae, are formed immediately after LPS addition and expand in size over the course of the video. Note, the overall fluorescence signal is reduced between images "6 s 652 ms" and "13 s 304 ms" (Series 1) because of slight defocusing of the sample due to the physical effect of adding the droplet of LPS at ~9 s. Refocusing on the sLBA after imaging reveals a similar sLBA fluorescence before and after LPS addition.